Journal of Inflammation Research

Dovepress
Taylor & Francis Group

Open Access Full Text Article

ORIGINAL RESEARCH

Effects of Electroacupuncture on Knee Osteoarthritis in Rats Through Suppressing p38 MAPK/ERK/CREB Pathway

Juan Wang[1,*], Fei Wang[1,*], Yiling Guo[2], Tun Liu[2], Jianxiong Li[3], Junbo Zou[4], Fei Luan[4], Tao Gao[5], Wei Wang[2]

[1]Department of Rehabilitation Medicine, Yulin Hospital, the First Affiliated Hospital of Xi'an Jiaotong University, Yulin, Shaanxi, 719000, People's Republic of China; [2]Comprehensive Orthopedics Department, the Second Affiliated Hospital of Xi'an Jiaotong University, Xi'an, Shaanxi, 710004, People's Republic of China; [3]The Second Ward of General Surgery, Yulin Hospital, The First Affiliated Hospital of Xi'an Jiaotong University, Yulin, Shaanxi, 719000, People's Republic of China; [4]Key Laboratory of Basic and New Drug Research in Chinese Medicine, Shaanxi University of Traditional Chinese Medicine, Xianyang, Shaanxi, 712046, People's Republic of China; [5]College of Acupuncture and Massage, Shaanxi University of Traditional Chinese Medicine, Xianyang, Shaanxi, 712046, People's Republic of China

*These authors contributed equally to this work

Correspondence: Wei Wang, Comprehensive Orthopedics Department, the Second Affiliated Hospital of Xi'an Jiaotong University, Xi'an, Shaanxi, 710004, People's Republic of China, Email dr.wangwei@xjtu.edu.cn

Purpose: Knee osteoarthritis (KOA) is a chronic degenerative joint disease and recognized as the fourth leading cause of disability worldwide. Despite the proven clinical efficacy of electroacupuncture (EA) in alleviating KOA-related symptoms, the precise molecular mechanisms underlying its therapeutic effects remain incompletely elucidated. The purpose of this study is to determine and validate the potential therapeutic targets and mechanism of EA for KOA through a combined approach of in vivo experiments and transcriptomics analysis.

Methods: A total of 40 SD rats were randomly divided into four groups: control group, model group, two-course EA intervention group, and four-course EA treatment group. The KOA model was established with monosodium iodoacetate (MIA) intra-articular injection. The EA treatment groups received intervention at the Yanglingquan and Dubi acupoints. The control group received no intervention. All four groups underwent behavioral assessments (rat knee joint diameter and bilateral foot balance test), joint pathological analysis (Micro-CT and hematoxylin and eosin staining) to evaluate the effect of EA on KOA. Transcriptomics, GO analysis and KEGG analysis were applied to predict potential targets. Potential targets were further verified via Western blot (WB).

Results: EA could significantly reduce knee joint diameters and improve the supporting force of KOA rats. Micro-CT revealed that EA increased the subchondral bone mass of KOA rats. ELISA results suggest that the levels of interleukin-1β and tumor necrosis factor-α decreased after EA intervention. The transcriptomics analysis revealed that EA could downregulate the levels of phospho (p)-p38 mitogen-activated protein kinase (MAPK), p-extracellular signal-regulated kinase (ERK), and p-cAMP response element-binding protein (CREB) which is further verified via WB.

Conclusion: EA intervention significantly ameliorated KOA-induced degeneration of cartilage and subchondral bone, improved pain-associated behavioral performance, alleviated inflammation. The molecular mechanism is related to the inhibition of the p-p38 MAPK/ERK/CREB pathway.

Keywords: knee osteoarthritis, electroacupuncture, in vivo experiments, transcriptomics, p38 MAPK/ERK/CREB pathways

Introduction

Knee osteoarthritis (KOA) is the most prevalent chronic degenerative joint disease worldwide. With the increase in the elderly population, its incidence and disability rate have both significantly risen.[1] According to global epidemiological data from 2021, approximately 2.5 billion individuals suffer from osteoarthritis (OA) worldwide, with KOA accounting for 85% of these cases. Among individuals aged 60 and above, about 18% of women and 9.6% of men are affected by

https://doi.org/10.2147/JIR.S581985
Received: 24 December 2025
Accepted: 14 April 2026
Published: 13 May 2026

this condition.[2] The pathogenesis of KOA is intricate, encompassing a multitude of factors such as inflammatory cytokines, degradation of the extracellular matrix, growth factors, and phospho (p)-p38 mitogen-activated protein kinase (MAPK)/extracellular signal-regulated kinase (ERK)/cAMP response element-binding protein (CREB) pathways. The core pathological features of KOA include cartilage degeneration, synovial inflammation, abnormal subchondral bone remodeling, and neuropathic pain.[3,4] The p38 MAPK/ERK/CREB signaling pathway is a core pathway that regulates cell proliferation, differentiation, inflammatory responses, and neural signal transduction.[5] Under normal physiological conditions, p38 MAPK (in the resting state) is the main form within cells. When the body is stimulated, the specific sites of p38 MAPK can be phosphorylated, transforming it into p-p38 MAPK (activated state) and initiating downstream signal transduction. The excessive activation of the p-p38 MAPK/ERK/CREB signaling pathway can lead to increased expression of inflammatory cytokines (such as [Interleukin, IL]-1β, [Tumor Necrosis Factor, TNF]-α, IL-6) and matrix degrading enzymes in chondrocytes, thereby exacerbating the destruction of cartilage.[6] It can also promote chondrocyte apoptosis through endoplasmic reticulum stress and reactive oxygen species.[7] Inhibiting p38 MAPK can enhance autophagy in chondrocytes by blocking the p38 MAPK/ERK/CREB signaling pathway, thereby preventing the progression of OA.[8] Clinically, patients often present with knee pain, swelling, joint stiffness, restricted movement, and even joint deformities. These changes not only lead to functional impairments of the knee joint but also severely impact the quality of life of patients.

At present, for patients with mild to moderate KOA, physical therapy applications, injections, orthotics, oral and topical medications are commonly used as conservative treatments, which can effectively relieve pain and improve functional conditions.[9] However, the long-term use of non-steroidal drugs may lead to adverse reactions such as gastrointestinal bleeding, perforation and cardiovascular diseases.[10] For patients with severe cartilage wear in the later stage, total knee replacement surgery is the main treatment option, but it often affects the prognosis due to accompanying chronic postoperative pain and is also costly.[11] Therefore, it is crucial to intervene as early as possible with more effective, safer and more economical treatment methods and to preserve the patient's original knee joint.

Traditional Chinese Medicine (TCM) treatments for KOA are receiving increasing attention due to more significant efficacy, fewer adverse reactions, and a much more broad scope of application.[12] Low-level laser therapy on acupuncture points has also become a research hotspot in the treatment of KOA due to its direct effect and low side effects. It can effectively alleviate the knee pain and joint function of KOA patients.[13] In recent years, Electroacupuncture (EA), a TCM treatment method that uses electrical stimulation on acupuncture points, has gradually attracted attention and demonstrated unique advantages in the treatment of KOA.[14,15] EA is a therapeutic method that integrates traditional acupuncture with modern electrostimulation technology. By stimulating acupuncture points, it not only promotes the release of analgesic substances,[16,17] but also induces muscle contraction, adjusts muscle tone and improves local blood circulation. Eventually, tissue repair is promoted. Previous studies suggest EA could alleviate knee pain, improve joint function, mitigate inflammation, prevent cartilage and subchondral bone degeneration.[18–23] However, the specific mechanisms of EA relieving KOA-related pain have not yet been fully elucidated.

In this study, we established KOA model with MIA, collected spinal cord samples. The transcriptomics technology was applied to screen potential targets for EA in improving KOA, and in vivo experiments were conducted to identify the mechanism of EA in treating KOA.

Materials and Methods

Materials

Disposable Sterile Acupuncture Needles (Guizhou Yunlong Medical Technology Co., Ltd.; Batch No.: 2405281); Sterile Insulin Syringes (Shanghai Kangdailai Enterprise Development Co., Ltd).; Bilateral Foot Balance Algometer (IITC Life Science, Model No.: 123019–600); Microplate Reader (Thermo Scientific, Model No.: 51119670DP); Micro-CT (SKYSCAN-1276, Serial No.: 19G17070); Upright Optical Microscope (Nikon Eclipse E100, Japan); Huatuo SD-II Type EA Device (SDK0052, Suzhou Medical Supplies Factory Co., Ltd).; Imaging System (Nikon DS-U3, Japan); High-Speed Low-Temperature Tissue Grinder (Wuhan Servicebio Technology Co., Ltd.; Model No.: KZ-III-F); Protein Electrophoresis and Chemiluminescence Imaging System (Bio-Rad ChemiDoc XRS; USA); Sodium Iodoacetate

(Shanghai Yuanye Biotechnology Co., Ltd.; Batch No.: K25036); Rat IL-1β ELISA Kit (MM-0045R1); Rat TNF-α ELISA Kit (MM-0201R1); Phospho-ERK Rabbit pAb (310065), Phospho-p38 Rabbit pAb (310069), Phospho-CREB Rabbit mAb (340731), ERK (343830), p38 (R25239), and CREB Ab (R23983) were all purchased from Chengdu Zenbioscience; BCA Assay Kit, HRP Conjugated AffiniPure Goat Anti-mouse IgG (H+L) (BST18K21C18K53), GAPDH (17L02A24④), and HRP Conjugated AffiniPure Goat Anti-rabbit IgG (H+L) (BST18F26C18G56) were all purchased from Boster Biological Technology.

Animals

Adult female Sprague-Dawley (SD) rats (180–200 g) were obtained from Chengdu Dashuo Experimental Animal Co., Ltd. All rats lived in an SPF-grade environment with a temperature of 22±1°C and relative humidity of 55±5%, a light-dark cycle of 12 h, and an adequate supply of food and water. The rats were anesthetized with isoflurane and euthanized with carbon dioxide. This study adheres to ARRIVE guidelines.

Establishment of MIA-Induced KOA Model

A total of 40 rats were randomly divided into control group, model group, two-course EA intervention group and four-course EA intervention group, with 10 rats in each group. All rats, except control group, received MIA intra-articular injection.[24] In short, 50 μL of 60 mg/mL MIA solution was injected into the left knee joint cavity on day 1, 4, and 7 to induce KOA model. If the diameter of left knee joint is 20% larger than that of the right knee joint, the KOA model is considered successful.[25]

EA Procedures

After 14 days of modeling, EA was performed on all EA groups. The rats were fixed during the intervention period, disposable sterile acupuncture needles (0.18 mm×13 mm) were used to pierce the Yanglingquan and the Dubi (Lateral genicular eye) on the left knee. Yanglingquan is located at the lateral and inferior part of the knee joint and the depression of the anterior and inferior part of the capitulum fibula of the lateral leg and the Dubi acupoint is located in front of the knee joint.[26,27] The two needles were then connected to the electrical stimulator (SDZ-II). The EA parameters were set as follows: alternating 2/100 Hz, dense-sparse wave, intensity < 2 mA, each session lasted 15 minutes, once daily, with five sessions constituting one course of treatment (Figure S1).

Behavioral Tests

Knee Joint Diameter Measurement

The diameters of the knee joints were measured using a digital caliper on the day before modeling, the third, seventh, and fourteenth days after modeling, as well as after the fifth, tenth, and twentieth EA interventions.

Bilateral Foot Balance Test

The supporting force of the hind paw was measured using a bilateral foot balance algometer on the day before modeling, the third, seventh, and fourteenth days after modeling, as well as after the fifth, tenth, and twentieth EA interventions.

Histopathological Examination of Joints

Micro-CT

After the final EA intervention, the rats were weighed, fasted for 12 hours (with water), and anesthetized with 3% sodium pentobarbital (1 mL/kg). The tibia was harvested and analyzed using micro-CT to assess the subchondral bone microstructure.

Hematoxylin and Eosin (HE) Staining

The tibia was fixed in 4% paraformaldehyde, decalcified and dehydrated routinely, and embedded in paraffin. After dewaxing and rehydration, the sample was cut into slices. The slices were stained with hematoxylin and eosin and observed under a microscope.

Transcriptomic Analysis of EA Treatment for KOA

Preparation and Detection of Transcriptomic Samples

RNA was extracted from the collected spinal cord tissue samples and subjected to quality assessment. The extracted mRNA was enriched using mRNA Capture Beads. After purification with magnetic beads, the mRNA was fragmented by applying high temperature. Subsequently, the first strand of cDNA was synthesized using the fragmented mRNA as a template. During the synthesis of the second strand of cDNA, end repair and addition of A-tails were performed simultaneously. Adapters were then ligated, and target fragments were purified using Hieff NGS® DNA Selection Beads. PCR amplification of the library was subsequently carried out. After the sequencing library passed quality control, sequencing analysis was performed.

Differential Gene Expression Analysis

HTSeq (version 0.9.1) was used to count the number of reads mapped to each gene, which served as the raw expression level. To make gene expression levels comparable across different genes and samples, the expression values were normalized using FPKM (Fragments Per Kilobase of transcript per Million mapped reads). FPKM represents the number of fragments per million mapped reads that originate from each kilobase of a gene's length. For paired-end sequencing, each fragment consists of two reads, and FPKM only counts the number of fragments where both reads can be mapped to the same transcript. Differential expression analysis was conducted using DESeq software (version 1.20.0) to compare gene expression levels between two groups. Genes with a fold change [$\log_2$(FC)] greater than 2 and a significance level of $P<0.05$ were identified as differentially expressed genes and were selected for further analysis.

Transcriptomic Enrichment Analysis

The differentially expressed genes from each group were analyzed using the Omicsmart analysis platform and the Omicshare online analysis platform (https://www.omicshare.com/tools/Home/Soft/ getsoft) for GO and KEGG analyses to identify the core signaling pathways affected in the spinal cord.

ELISA Detection of Inflammatory Factors

After completing EA intervention, the rats were weighed, fasted for 12 hours (with water), and anesthetized with 10% sodium pentobarbital (1 mL/kg). The skin was incised along the midline of the back, the muscles were separated, and the vertebrae were exposed. The L3-L5 location was identified, the lamina was removed, and the spinal cord was exposed. The nerve roots were cut, and the left spinal cord tissue was removed and placed in a pre-cooled preservation solution. The levels of IL-1β and TNF-α were measured using ELISA kits according to the manufacturer's instructions to evaluate the anti-inflammatory effects of the treatment.

Western Blotting (WB)

The spinal cord tissue was ground with liquid nitrogen. After thorough grinding, protein lysis buffer, protease inhibitors, and phosphatase inhibitors were added. The mixture was left to incubate on ice for 15min, followed by centrifugation at 12000 rpm for 15min at 4°C. The supernatant from each group was then quantified using BCA. Subsequently, sample loading, electrophoresis, transfer, and blocking were carried out, followed by incubation with primary antibodies according to the antibody instructions for p-ERK (1:2000), p-p38 MAPK (1:2000), p-CREB (1:2000), ERK (1:2000), p38 (1:2000), CREB (1:2000) and GAPDH (1:5000) at 4°C overnight. After washing the membrane with TBST, it was incubated with secondary antibodies rabbit (1:5000) and mouse (1:5000) at room temperature for 2h. ECL chemiluminescent detection reagent was used for development, and Image J software was utilized to quantitatively analyze the absorbance of protein expression bands.

Statistical Analysis

Data analysis was performed using SPSS 20.0 software. All experiments were repeated 3 times, and the measurement data were presented in the form of mean ± standard deviation ($\overline{X} \pm SD$). Perform the Shapiro–Wilk normality test on all the data. For data that follow a normal distribution and have homogeneity of variance, the unpaired *t*-test is used to compare the mean differences between two independent groups, while one-way analysis of variance (ANOVA) is employed to compare the overall mean differences among multiple groups. For pairwise comparisons, if the homogeneity

of variance was present, the LSD-*t* test was used; otherwise, Tamhane's T2 test was employed. Mann–Whitney *U*-test for non-normally distributed data. The significance level was set at $P<0.05$, indicating a statistically significant difference.

Results

EA Alleviated Knee Joint Swelling in KOA Rats

Measurements of knee joint diameter revealed that the knee joint diameter in the model group significantly increased at 3, 7, and 14 days after modeling ($P<0.01$) (Table 1 and Figure 1A [a]), indicating successful establishment of KOA model. After EA treatment, the knee joint diameter in both the two-course and four-course groups significantly decreased ($P<0.01$), with the four-course group showing a more notable reduction ($P<0.01$). These results indicate that EA effectively alleviated MIA-induced knee joint swelling.

EA Improved the Weight-Bearing Capacity of MIA-Induced KOA

The results of the bilateral foot balance test indicated that, compared with the control group, the supporting force of the left hind paw in the model group significantly decreased at 3, 7, and 14 days after modeling ($P<0.01$). After EA treatment, the supporting force of the left hind paw in both the two-course and four-course groups significantly increased ($P<0.01$), with the four-course group showing a more notable increase ($P<0.01$). These results indicate that EA treatment significantly improved hind paw weight-bearing capacity (a pain-associated behavioral indicator) in KOA rats[28] (Table 2 and Figure 1A [b]).

EA Attenuated the Subchondral Bone Degeneration of MIA-Induced KOA

To investigate the effect of EA on KOA knee joint structure, we examined the tibia using Micro-CT and performed quantitative analysis (Figure 1B). Quantitative analysis indicated that the model group exhibited significant subchondral bone osteoporosis manifesting as decreases in bone volume (BV), bone volume fraction (BV/TV), bone surface area to tissue volume ratio (BS/TV), trabecular thickness (Tb.Th), trabecular number (Tb.N), and degree of anisotropy (DA) and increases in bone surface area to bone volume ratio (BS/BV), trabecular pattern factor (Tb.Pf), structure model index (SMI), trabecular separation (Tb.Sp), connectivity (Conn), and connectivity density (Conn.Dn) ($P<0.05$). In terms of BV, BV/TV, Conn, BS/BV, the subchondral bone osteoporosis of the two-course EA group was reduced ($P<0.05$). However, there was no significant difference in Tb.Pf, SMI, Tb.Sp, and Conn.Dn ($P>0.05$). Compared with the model group and the two-course EA group, the four-course group exhibited more significant increases in bone mass, manifesting as more significant changes of bone indexes ($P<0.05$) (Figure 1C). These results indicate that EA attenuated the microstructural degeneration of the subchondral bone in KOA rats.

Table 1 Diameter of the Rat Knee Joint ($\overline{X} \pm SD$, n=10, mm)

	Control	Model	TC	FC
1d	14.72±0.57	15.01±0.35	15.10±0.10	15.09±0.11
3d	14.80±0.53	17.39±0.38**	17.42±0.48	17.54±0.49
7d	14.79±0.47	18.42±0.43**	18.16±0.30	18.32±0.26
14d	14.93±0.43	19.74±0.33**	19.50±0.46	19.55±0.29
5 times	14.92±0.38	19.80±0.24**	17.87±0.08##	17.93±0.06##
10 times	14.95±0.46	19.65±0.52**	16.69±0.09##	17.02±0.06##
20 times	14.93±0.47	19.43±0.85**	16.57±0.29##	16.27±0.04##

Note: Compared with the control group, **$P<0.01$; compared with the model group, ##$P<0.01$.

Abbreviations: 1d, One day before modeling; 3d, Three days after modeling; 7d, Seven days after modeling; 14d, Fourteen days after modeling; 5 times, 5 sessions of EA; 10 times, 10 sessions of EA; 20 times, 20 sessions of EA; TC, two courses of treatment; FC, four courses of treatment.

https://doi.org/10.2147/JIR.S581985

EA Ameliorates Knee Joint Pathological Lesions in MIA-Induced KOA

To determine whether EA alleviated knee joint pathological damage, we performed HE staining of knee joint sections (Figure 2A [a]). To enhance objectivity and reproducibility, histological changes were further evaluated using a predefined semi-quantitative scoring system that assessed inflammatory cell infiltration, edema, and structural damage (each graded 0–3, with a total score of 0–9; detailed criteria are provided in Supplementary Table S3). In the control group, the knee joint architecture was preserved, with orderly tissue arrangement and minimal inflammatory cell infiltration, corresponding to low histological scores. In contrast, the model group exhibited pronounced joint injury, characterized by indistinct tissue boundaries, marked edema, and prominent inflammatory cell infiltration, resulting in a significantly increased total histological score. Importantly, EA treatment mitigated these pathological alterations, as evidenced by reduced inflammatory infiltration and edema, improved tissue organization, and significantly lower histological scores compared with the model group (Figure 2A [b]). Collectively, the quantitative scoring results, together with representative HE images, indicate that EA attenuates knee joint pathological damage.

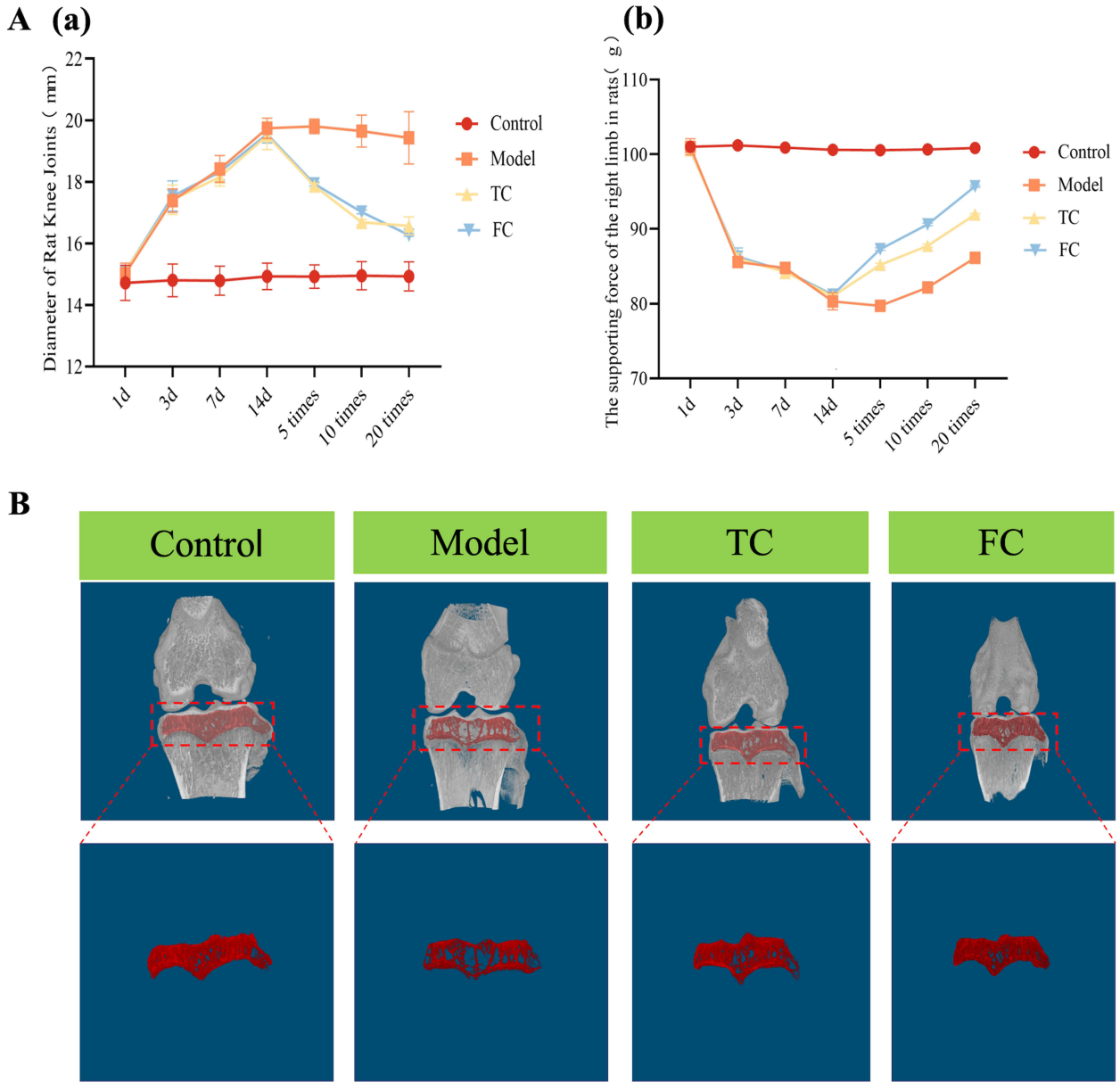

Figure 1 continued.

https://doi.org/10.2147/JIR.S581985

EA Alleviates Spinal Cord Inflammation in MIA-Induced KOA

As shown in Figure 2B, the levels of IL-1β and TNF-α of the KOA rats were significantly higher than those of the control group rats ($P<0.01$) which could be reduced by EA treatment ($P<0.01$). These results indicated that EA could effectively reduce the neural sensitization caused by inflammatory cytokines in KOA rats.

Spinal Cord Transcriptomic Profiling of EA-Treated MIA-Induced KOA Rats

To further determine the molecular mechanism of EA treatment, we performed transcriptome analysis on the left spinal cord of rats. As shown in Figure 3A [a–d], 701 differentially expressed genes (DEGs) were identified. Among all these DEGs, 29 related DEGs were found in all 4 groups (Figure 3A [e]). The complete gene list and corresponding statistical information are provided in Supplementary Table S1. The 29 key DEGs discussed in the main text are highlighted in red in this table. These related DEGs were subject to GO and KEGG analysis to determine their biological function and location. The 29 related DEGs were categorized into 33 functional classes, which was closely related to the localization, binding, and catalytic activity of proteins with complex molecular functions (Figure 3A [f]). KEGG enrichment analysis showed that EA treatment mainly involves pathways associated with Osteoclast differentiation, Relaxin signal, FcepsilonRI signal, and Hepatitis B (Figure 3A [g]). The significance metrics for each pathway (P values and FDR) are provided in Supplementary Table S2. Osteoclast differentiation pathway ranks first among all the related pathways.

EA Ameliorates KOA by Modulating Spinal Cord p38 MAPK/ERK/CREB Pathway

p38 MAPK/ERK/CREB pathway is well explored regarding osteoclast differentiation and pain. Additionally p38 MAPK/ERK/CREB pathway was found to participate in the pathogenesis of KOA. In order to explore the effect of EA on the

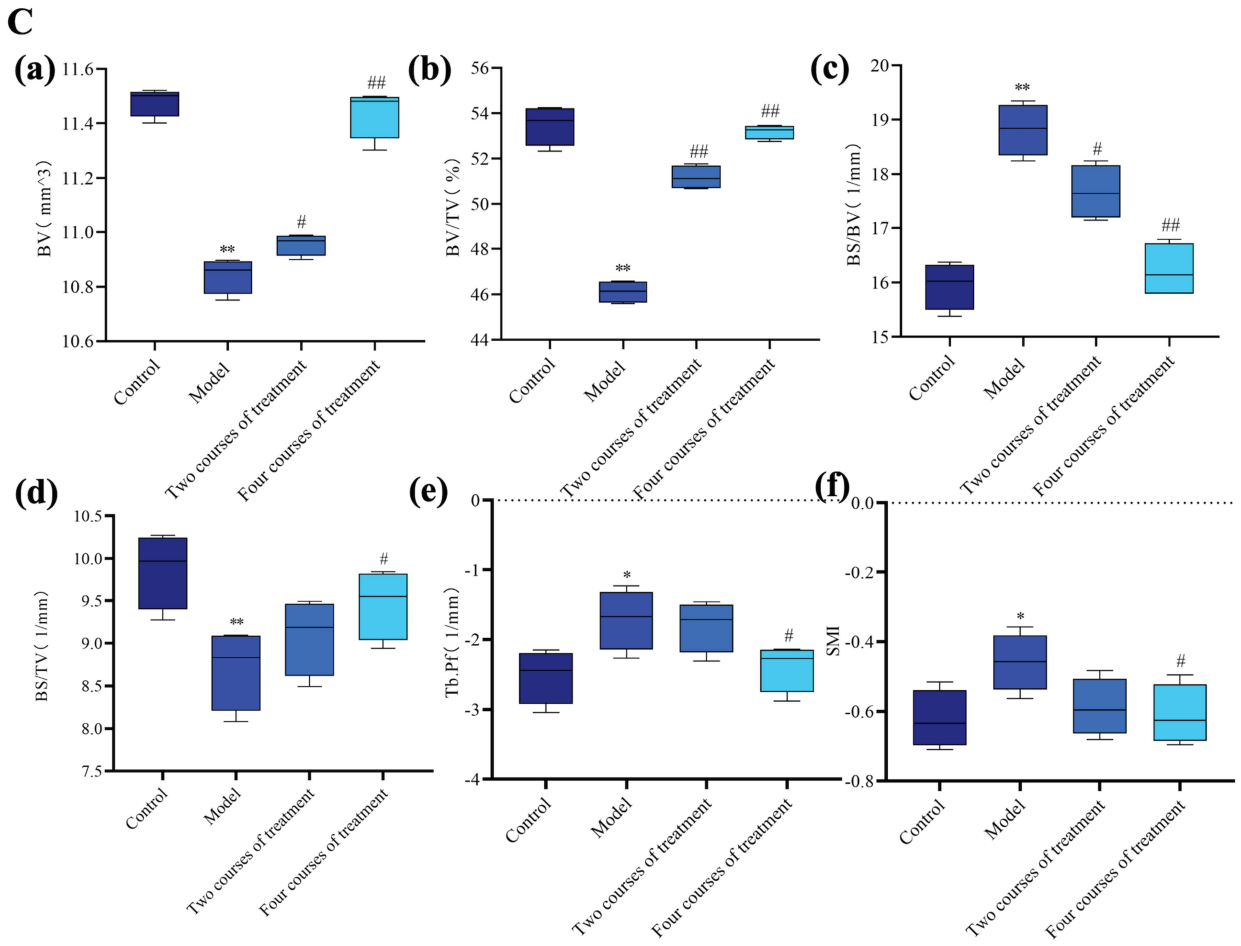

Figure 1 continued.

https://doi.org/10.2147/JIR.S581985

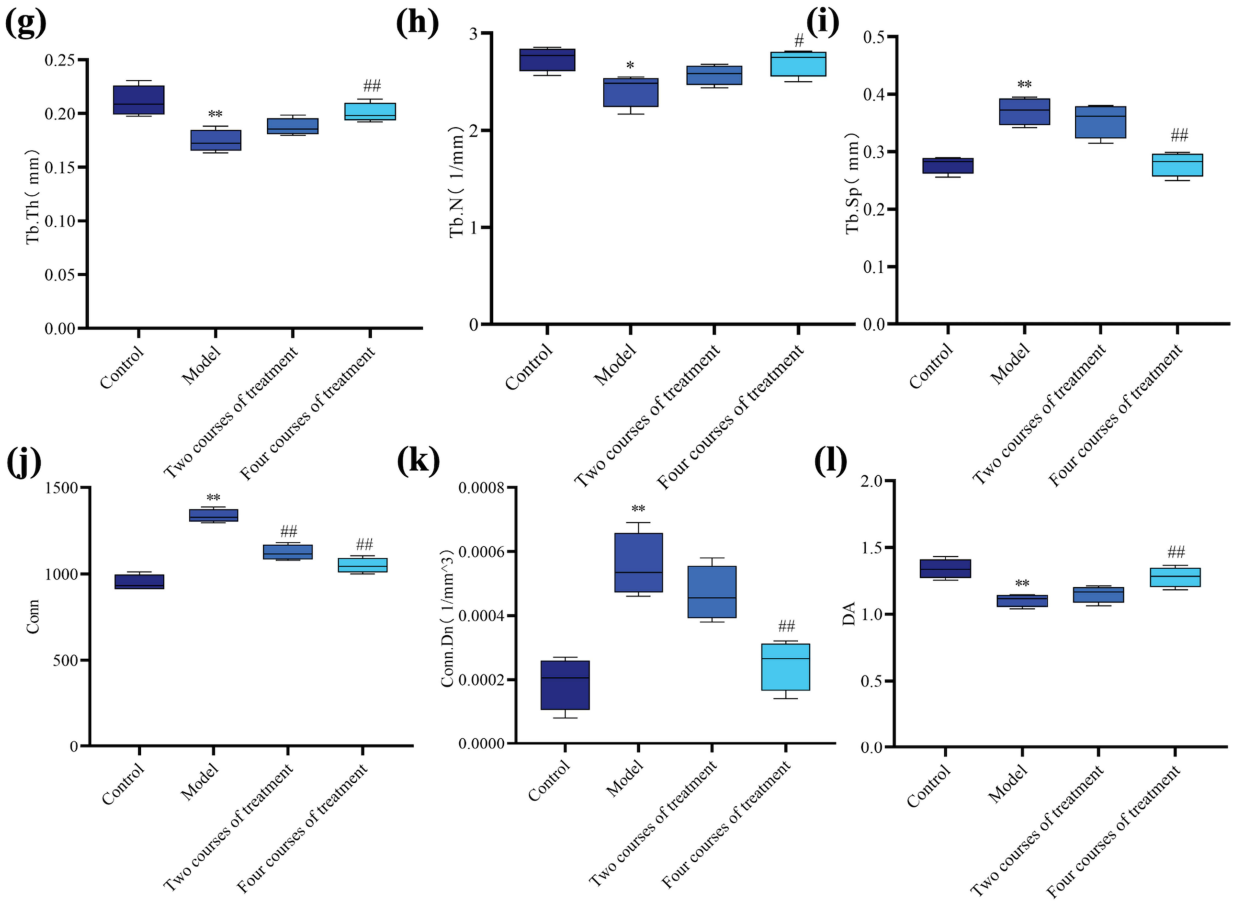

Figure 1 EA Ameliorates KOA-induced Pain, Swelling and Subchondral Bone Microstructural Pathological Changes in Rat Knee Joints. (**A**) Behavioral observation, with (a) showing changes in knee joint diameter, and (b) showing changes in the supporting force of the left limb (n=10) (compared with the control group, $^{**}P<0.01$; compared with the model group, $^{\#\#}P<0.01$). (**B**) Micro-CT assessment of joint pathological changes (n=4, red circles indicate the magnified areas). (**C**) EA attenuated the microstructural pathological changes of the subchondral bone in the rat knee joint. Micro-CT analysis results of the morphological parameters of subchondral bone microstructure in each group (n=4). (a) BV; (b) BV/TV; (c) BS/BV; (d) BS/TV; (e) Tb.pf; (f) SMI; (g) Tb.Th; (h) Tb.N; (i) Tb.Sp; (j) Trabecular Conn; (k) Trabecular Conn.Dn; (l) Trabecular DA (compared with the control group, $^{*}P<0.05$, $^{**}P<0.01$; compared with the model group, $^{\#}P<0.05$, $^{\#\#}P<0.01$).

Abbreviations: EA, electroacupuncture; 1d, One day before modeling; 3d, Three days after modeling; 7d, Seven days after modeling; 14d, Fourteen days after modeling; 5 times, 5 sessions of EA; 10 times, 10 sessions of EA; 20 times, 20 sessions of EA; TC, two courses of treatment; FC, four courses of treatment; BV, bone volume; BV/TV, bone volume fraction; BS/BV, Bone surface area to bone volume ratio; BS/TV, bone surface area to tissue volume ratio; Tb.Pf, trabecular pattern factor; SMI, structure model index; Tb.Th, trabecular thickness; Tb.N, trabecular number; Tb.Sp, trabecular separation; Conn, connectivity; Conn.Dn, connectivity density; DA, degree of anisotropy.

p-p38 MAPK/ERK/CREB signaling pathway, we measured the levels of p-ERK, p-p38 MAPK, and p-CREB in the left spinal cord of rats. As shown in Figure 3B [a–f], the expression levels of p-ERK, p-p38 MAPK, and p-CREB increased in the left spinal cord of the model group ($P<0.05$). EA reduced the phosphorylation levels of p-ERK, p-p38 MAPK, and p-CREB ($P<0.05$). These results indicated that EA can treat KOA via regulating the phosphorylation levels of p-p38 MAPK/ERK/CREB pathway.

Discussion

Therapeutic Effects of EA on KOA Rats: Multidimensional Validation

Our results demonstrated that EA intervention exerted comprehensive therapeutic effects on MIA-induced KOA rats, which was validated through behavioral, imaging, histopathological, and molecular biological assessments. Joint swelling is usually caused by fluid accumulation (abnormally increased fluid in the joint cavity) and/or edema (accumulation of fluid in the surrounding soft tissues of the joint).[29] The increase in the diameter of the knee joint directly reflects the degree of these pathological changes, and thus is regarded as an important clinical observation indicator. In terms of

Table 2 Supporting Force of the Left Hind Paw in Rats ($\overline{X} \pm SD$, n=10, g)

	Control	Model	TC	FC
1d	100.99±0.56	101.00±1.09	100.55±0.16	100.45±0.16
3d	101.20±0.31	85.55±0.41**	86.04±0.72	86.29±1.16
7d	100.89±0.19	84.77±0.64**	84.25±0.89	84.36±0.17
14d	100.60±0.18	80.31±1.14**	81.01±0.19	81.19±0.76
5 times	100.55±0.16	79.71±0.23**	85.18±0.21##	87.30±0.18##
10 times	100.65±0.16	82.15±0.23**	87.74±0.21##	90.60±0.18##
20 times	100.85±0.16	86.12±0.13**	91.92±0.15##	95.71±0.14##

Note: Data are expressed as $\overline{X} \pm SD$, compared with the control group, **P<0.01; compared with the model group, ##P<0.01.

Abbreviations: 1d, One day before modeling; 3d, Three days after modeling; 7d, Seven days after modeling; 14d, Fourteen days after modeling; 5 times, 5 sessions of EA; 10 times, 10 sessions of EA; 20 times, 20 sessions of EA; TC, two courses of treatment; FC, four courses of treatment.

behavioral outcomes, EA significantly reduced knee joint diameter (a direct indicator of joint swelling) in KOA rats. In the field of pain research, accurately and objectively assessing the pain behaviors of animal models serves as a bridge connecting basic research and clinical translation. Traditional pain assessment methods, such as the von Frey test, mainly measure induced pain (such as mechanical hyperalgesia or touch-induced pain).[30] However, in clinical cases of chronic pain, especially OA and postoperative pain, there are often significant components of spontaneous or weight-related pain.[28] In recent years, the measurement of hindlimb weight-bearing capacity, especially through dynamic or static weight-bearing tests, has become an important and sensitive behavioral indicator for evaluating non-induced pain or spontaneous pain in this type of condition.[31] This study found that EA can improve the pain condition of KOA rats by enhancing the weight-bearing capacity of the affected hindlimb on the KOA side. Notably, the four-course EA group showed more pronounced improvements than the two-course group, indicating a dose-dependent therapeutic effect of EA-consistent with clinical observations that prolonged and standardized EA intervention can bring better clinical effects to patients with KOA.[32] This dose-dependent effect may be attributed to the cumulative regulation of EA on pathogenic signaling pathways and inflammatory responses, which requires sufficient intervention duration to achieve optimal modulation.

Imaging analysis using Micro-CT revealed that EA effectively attenuated subchondral bone degeneration in KOA rats. Subchondral bone plays a crucial role in transmitting joint load and supporting cartilage; its degeneration exacerbates cartilage damage by altering mechanical stress distribution.[33] The model group exhibited significant subchondral bone osteoporosis, characterized by decreased BV, BV/TV, Tb.Th, and Tb.N, as well as increased Tb.Sp and SMI. These pathological changes are consistent with the disorder of subchondral bone remodeling in KOA.[34] EA intervention, especially with four courses of treatment, reversed these abnormalities, suggesting that EA can regulate subchondral bone degeneration to maintain bone microstructural integrity.

Histological examination with HE staining further confirmed that EA mitigated cartilage degeneration in KOA rats. The model group showed typical KOA pathological features, including narrowed joint space, disrupted cartilage surface, and inflammatory cell infiltration, while EA treatment significantly ameliorated these changes. This chondroprotective effect of EA is consistent with previous studies reporting that EA can inhibit chondrocyte apoptosis, promote extracellular matrix synthesis, and suppress cartilage degradation.[35] The research suggests that the reduction in limb weight-bearing, the degree of swelling, and the local expression of inflammatory mediators are all related.[28,30] Additionally, ELISA results indicated that EA reduced the levels of pro-inflammatory cytokines IL-1β and TNF-α in the spinal cord of KOA rats. IL-1β and TNF-α are key mediators of KOA pathogenesis, as they not only induce synovial inflammation but also promote the expression of matrix metalloproteinases (MMPs) to accelerate cartilage degradation and lower the pain threshold by sensitizing spinal cord neurons.[36] The downregulation of IL-1β and TNF-α by EA may therefore contribute to both anti-inflammatory and analgesic effects.

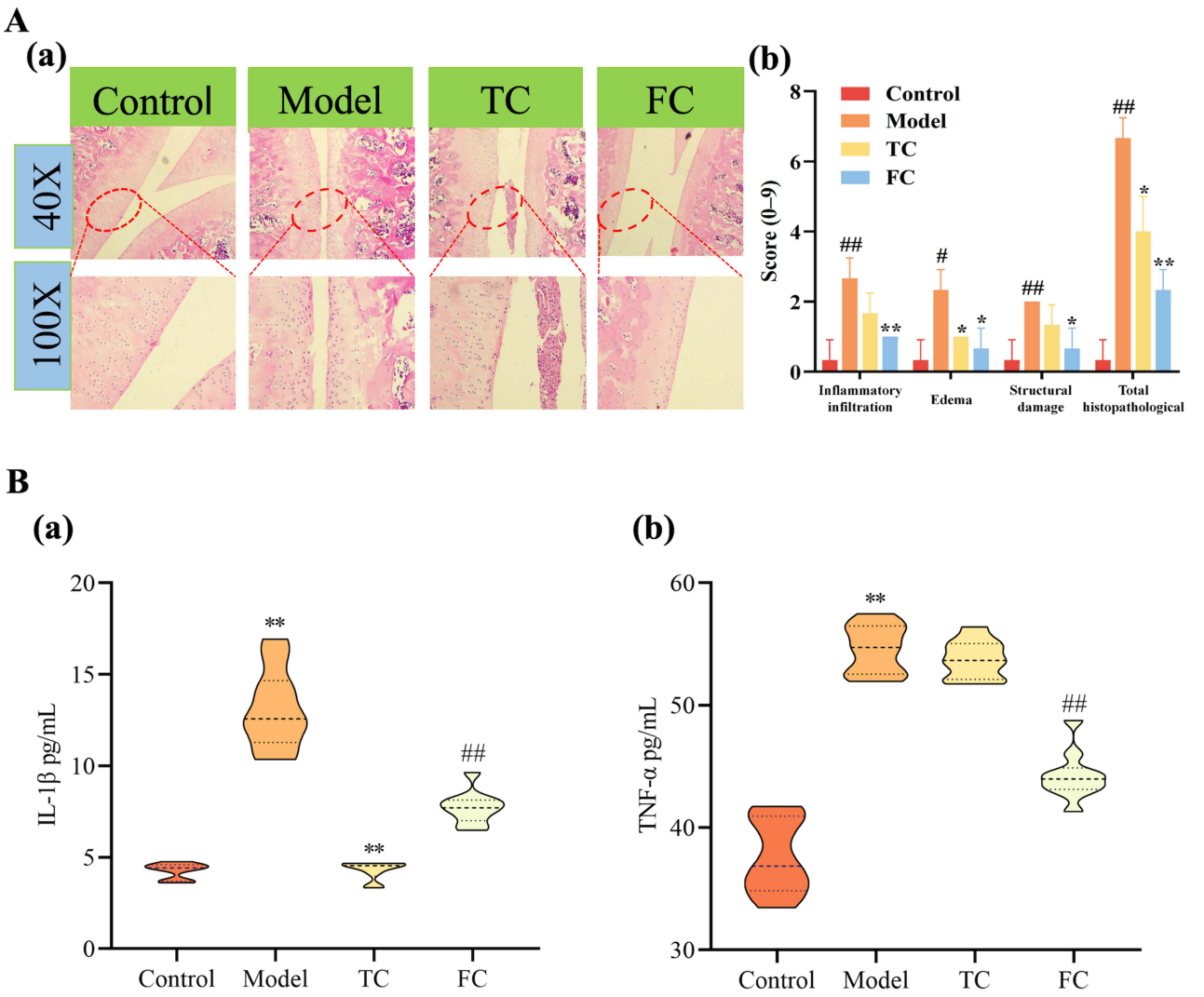

Figure 2 EA Improves Knee Joint Pathological Structure and Attenuates Spinal Cord Inflammation in KOA Rats. (**A**) EA attenuated the pathological changes of the cartilage in the knee joint of rats. (a) HE staining shows the subchondral bone region of the joint, (b) Histopathological scores of knee articular cartilage in each group, including inflammatory infiltration, edema, structural damage, and total histopathological score. Data are presented as $\overline{X} \pm SD$ (n=3). (scale bars 10 μm and 20 μm, n=3; red circles indicate the magnified areas; compared with the model group, **P*<0.05, ***P*<0.01; compared with the control group, $^{\#}P$<0.05, $^{\#\#}P$<0.01. (**B**) EA Suppresses the Expression of Spinal Cord Inflammatory Cytokines in KOA Rats. (a) IL-1β, (b) TNF-α (n=10). Data are expressed as mean ± SD, compared with the control group, ***P*<0.01; compared with the model group, $^{\#\#}P$<0.01.

Abbreviations: EA, electroacupuncture; HE, Hematoxylin and eosin; IL-1β, Interleukin-1β; TNF-α, Tumor Necrosis Factor-α; TC, two courses of treatment; FC, four courses of treatment.

Underlying Molecular Mechanisms: Regulation of the p38 MAPK/ERK/CREB Pathway

Previous studies have revealed the multifaceted mechanisms of EA. First, EA induces analgesic effects via the endogenous opioid peptide system, which inhibits pain signal transmission.[37] Second, EA modulates neurotransmitters such as serotonin and norepinephrine, thereby improving neural function and alleviating neuropathic pain.[38] p38 MAPK/ERK/CREB pathway, a previously confirmed pathway involving osteoclast differentiation during KOA,[39] is also a common pathway regarding pain. In our study, we first found that p38 MAPK/ERK/CREB pathway is also involved in chronic KOA neural pain and could be one of the EA pain relieving mechanisms. Previous study identified P2X4 receptor as a key target of EA pain relieving.[40] Herein, we found a new mechanism of EA pain relieving.

To further explore the molecular mechanisms of EA's therapeutic effects, we performed transcriptomic analysis on spinal cord tissues of KOA rats. KEGG enrichment analysis of DEGs identified the osteoclast differentiation pathway as the most significantly enriched pathway, which is closely associated with the p38 MAPK/ERK/CREB signaling pathway

—known to be involved in osteoclast differentiation and pain modulation.[39] WB validation confirmed that EA significantly reduced the phosphorylation levels of p38 MAPK, ERK, and CREB in the spinal cord of KOA rats, while the total protein levels of these molecules remained unchanged, indicating that EA exerts its effects through the dephosphorylation of key kinases in this pathway.

Rationale for Selecting Yanglingquan and Dubi Acupoints

The selection of Yanglingquan (GB34) and Dubi (ST35) acupoints in this study was grounded in their anatomical proximity, neurophysiological effects, and demonstrated therapeutic outcomes in clinical and preclinical studies. Anatomically, Yanglingquan is a distal point on the Gallbladder Meridian, it is traditionally associated with tendon and joint disorders. Its location near the fibular head allows modulation of peripheral nerves (eg, common peroneal nerve), influencing knee stability and pain pathways.[41] Stimulating Yanglingquan can dredge meridians, relieve pain, and

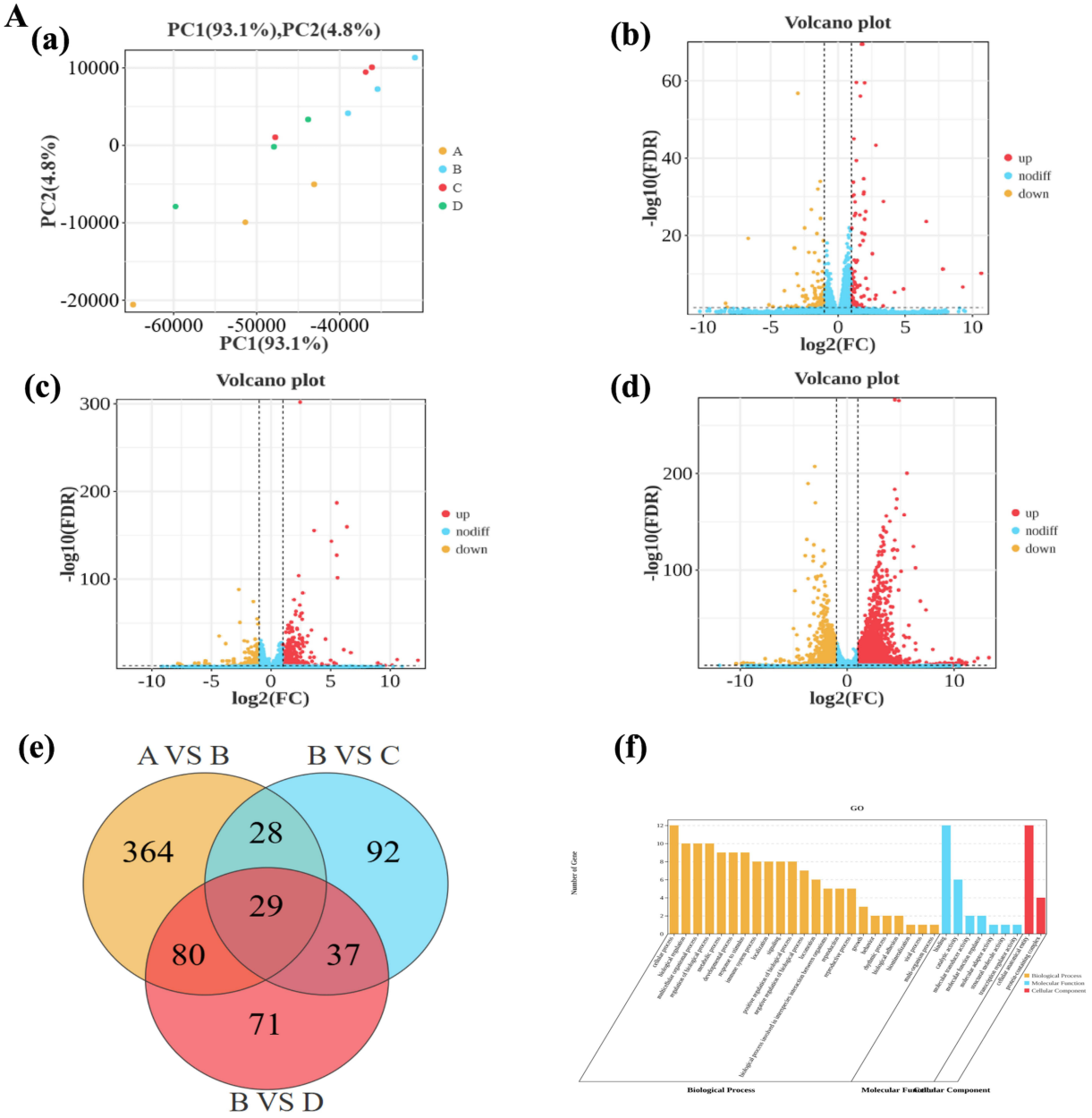

Figure 3 continued.

https://doi.org/10.2147/JIR.S581985

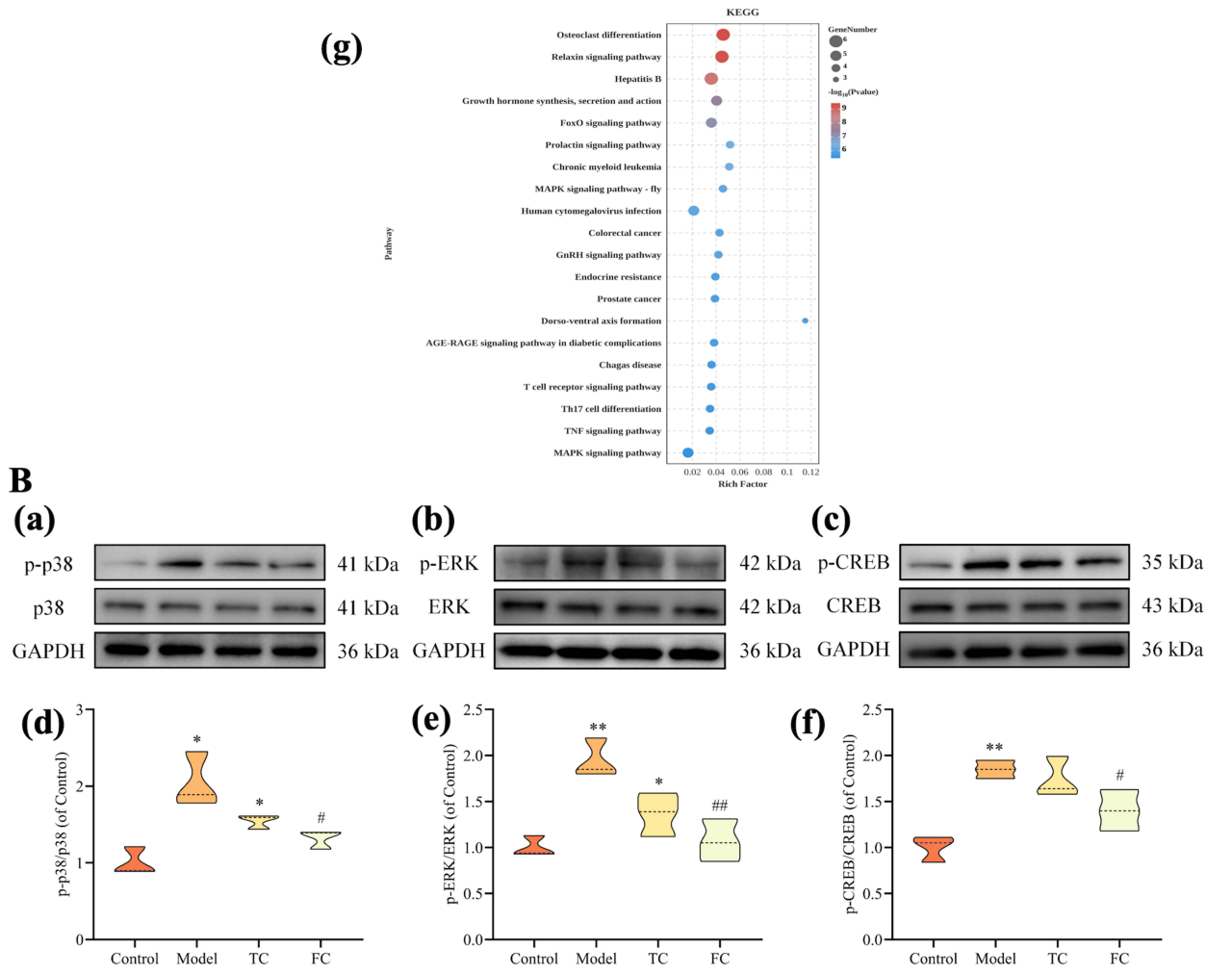

Figure 3 EA Ameliorates KOA by Regulating the p38 MAPK/ERK/CREB Signaling Pathways in Rats. (**A**) Transcriptomic Profiling of KOA Rats Following EA Intervention. (a) PCA among the control group, model group, and treatment groups in the EA-treated KOA rat model (A: Control; B: Model; C: TC; D: FC). (b)-(d) Volcano plots of differentially expressed genes between the EA-treated KOA rat model group and the control group, the model group and TC, and the model group and FC. (e) Venn diagram of commonly expressed genes between the EA-treated KOA rat model group and the control group, the model group and TC, and the model group and FC. (f) GO analysis of commonly expressed differentially regulated genes in EA-treated KOA rats. (g) KEGG analysis of commonly expressed differentially regulated genes in EA-treated KOA rats. (**B**) EA Regulates Spinal Cord p38 MAPK/ERK/CREB Pathway Protein Expression in KOA Rats. (a)-(f): The protein expression of p-38, p-ERK, and p-CREB was detected by WB, with GAPDH serving as the internal control (n=3). Data are expressed as $\overline{X} \pm SD$ compared with the control group, **P*<0.05, ***P*<0.01; compared with the model group, $^{\#}P$<0.05, $^{\#\#}P$<0.01.

Abbreviations: EA, electroacupuncture; KOA, knee osteoarthritis; MAPK, mitogen-activated protein kinase; p, phospho; ERK, extracellular signal-regulated kinase; CREB, cAMP response element-binding protein; PCA, Principal Component Analysis; EA, electroacupuncture; TC, two courses of treatment; FC, four courses of treatment; GO, Gene Ontology; KEGG, Kyoto Encyclopedia of Genes and Genomes; p, phospho; WB, Western blot.

strengthen tendons and bones. Dubi is located at the knee's depression lateral to the patellar ligament, it is a local point directly targeting the affected joint. Its selection aligns with the principle of "treating local disorders with nearby acupoints" in TCM, it acts by dredging local meridians and collaterals, reducing swelling, and alleviating pain.[42] Clinically, these two acupoints are widely used in the treatment of KOA and have been validated by numerous studies. A data mining analysis of acupuncture for KOA found that Yanglingquan and Dubi are among the most frequently used acupoints, with significant efficacy in improving joint pain and function.[43] Additionally, previous studies have shown that EA at Yanglingquan and Dubi can regulate the expression of inflammatory factors and pain-related signaling pathways in KOA models,[22] providing a solid experimental basis for their selection in this study.

Strengths and Limitations of the Study

Strengths

Firstly, this study employed a comprehensive research design integrating behavioral tests, Micro-CT, HE staining, transcriptomics, ELISA, and WB, which systematically validated the therapeutic effects of EA on KOA from multiple dimensions. Secondly, we identified the p38 MAPK/ERK/CREB pathway as a key target of EA, providing a novel molecular mechanism for the analgesic and chondroprotective effects of EA in KOA. Thirdly, the study investigated the dose-dependent effect of EA by comparing two-course and four-course interventions, which offers valuable insights for clinical practice. Finally, the selection of acupoints was based on a combination of TCM theory and clinical evidence, enhancing the translational potential of the results.

Limitations

Despite these strengths, several limitations should be acknowledged. Firstly, this study was conducted in a rat model, and the results may not fully translate to human KOA-future clinical studies are needed to validate the regulation of the p38 MAPK/ERK/CREB pathway by EA in KOA patients. Secondly, while we demonstrated that EA dephosphorylates p38 MAPK/ERK/CREB, the specific phosphatases involved and the upstream regulatory mechanisms remain unclear, requiring further investigation using phosphatase inhibitors or gene silencing techniques. Thirdly, the study focused on spinal cord tissues, and the effects of EA on other relevant tissues (eg, synovium, cartilage, subchondral bone) and joint range of motion have not been evaluated—future studies should analyze multiple tissues to comprehensively understand the systemic regulatory effects of EA. Fourthly, weight-bearing on the affected limb is an indirect measure of pain, and future studies should incorporate direct pain assessment methods to provide more robust evidence of EA's analgesic effect.

Conclusion

This study revealed that EA intervention can significantly restore osteochondral structure, improve the behavioral manifestations related to pain and reduce inflammation. These effects can be achieved by inhibiting the p-p38 MAPK/ERK/CREB pathway. These findings suggest that EA may be a new safe option for the etiological treatment of KOA.

Abbreviations

EA, Electroacupuncture; FC, Four courses of treatment; HE, Hematoxylin and eosin; IL-1β, Interleukin-1β; KOA, Knee osteoarthritis; MIA, Monosodium iodoacetate; NSAIDs, Nonsteroidal anti-inflammatory drugs; OA, Osteoarthritis; p-CREB, Phosphorylated cAMP response element-binding protein; p-ERK, Phosphorylated extracellular signal-regulated kinase; p-p38, Phosphorylated p38; TC, Two courses of treatment; TCM, Traditional Chinese Medicine; TNF-α, Tumor necrosis factor-α.

Data Sharing Statement

Raw data were generated at Shaanxi University of Traditional Chinese Medicine. Derived data supporting the findings of this study are available from the corresponding author WW on reasonable request.

Ethics Approval

All animal experiments were approved by the Animal Ethics Committee of Shaanxi University of Chinese Medicine (No. SUCMDL20240820006) and performed in compliance with the National Institutes of Health Guide for the Care and Use of Laboratory Animals (2022-K-30).

Consent for Publication

All authors confirm that the details of any images, videos, recordings, etc can be published, and consent to publish. All authors agree to be accountable for all aspects of work ensuring integrity and accuracy.

Acknowledgments

The authors would like to thank National Natural Science Foundation of China, Shaanxi government and Yulin government for their generous funding. We thank Prof. Zhengquan Lei for his suggestion regarding the experiment. The authors thank Key Laboratory of Basic and New Drug Research in Chinese Medicine for their assistance with the experiment.

Author Contributions

Juan Wang: Conceptualization, Methodology, Formal analysis, Writing - original draft

Fei Wang: Conceptualization, Methodology, Writing - original draft

Yiling Guo: Methodology, Visualization, Writing – original draft, Writing – review & editing

Tun Liu: Methodology, Visualization, Writing – original draft

Jianxiong Li: Formal analysis, Writing – original draft

Junbo Zou: Conceptualization, Methodology, Writing – original draft

Fei Luan: Formal analysis, Writing – review & editing

Tao Gao: Funding acquisition, Supervision, Writing – review & editing

Wei Wang: Funding acquisition, Supervision, Writing – review & editing

All authors gave final approval of the version to be published; have agreed on the journal to which the article has been submitted; and agree to be accountable for all aspects of the work.

Funding

This work was supported by the National Natural Science Foundation of China (No. 81804162), the Key Research Project of Shaanxi Province (2024SF-YBXM-498 and 2025SF-YBXM-153) and Yulin talents project (2024-KJZG-ZQNLJ-006).

Disclosure

The authors declare that there are no conflicts of interest.

References

1. Xie X, Zhang K, Li Y, et al. Global, regional, and national burden of osteoarthritis from 1990 to 2021 and projections to 2035: a cross-sectional study for the global burden of disease study 2021. *PLoS One*. 2025. doi:10.1371/journal.pone.0324296
2. Quicke JG, Conaghan PG, Corp N, Peat G. Osteoarthritis year in review 2021: epidemiology & therapy. *Osteoarthritis Cartilage*. 2021. doi:10.1016/j.joca.2021.10.003
3. Felson DT. Osteoarthritis: priorities for osteoarthritis research: much to be done. *Nat Rev Rheumatol*. 2014;10(8):447–448. doi:10.1038/nrrheum.2014.76
4. Eymard F, Chevalier X. Inflammation of the infrapatellar fat pad. *Joint Bone Spine*. 2016;83(4):389–393. doi:10.1016/j.jbspin.2016.02.016
5. Crown ED, Ye Z, Johnson KM, Xu G-Y, McAdoo DJ, Hulsebosch CE. Increases in the activated forms of ERK 1/2, p38 MAPK, and CREB are correlated with the expression of at-level mechanical allodynia following spinal cord injury. *Exp Neurol*. 2006;199(2):397–407. doi:10.1016/j.expneurol.2006.01.003
6. Li H, You Y, Jiang B, et al. Wang-Bi Tablet ameliorates DMM-induced knee osteoarthritis through suppressing the activation of p38-MAPK and NF-κB signaling pathways in mice. *Evid Based Complement Alternat Med*. 2021;2021:1–9. doi:10.1155/2021/3930826
7. Lu J, Yu M, Li J. PKC-δ promotes IL-1β-induced apoptosis of rat chondrocytes and via activating JNK and P38 MAPK pathways. *Cartilage*. 2023;15(3):315–327. doi:10.1177/19476035231181446
8. Wei J, You G, Cheng H, Gao C. SPRED2 promotes autophagy and attenuates inflammatory response in IL-1β induced osteoarthritis chondrocytes via regulating the p38 MAPK signaling pathway. *Tissue Cell*. 2023;82:102086. doi:10.1016/j.tice.2023.102086
9. Deyle GD, Allen CS, Allison SC, et al. Physical therapy versus glucocorticoid injection for osteoarthritis of the knee. *N Engl J Med*. 2020;382(15):1420–1429. doi:10.1056/NEJMoa1905877
10. Primorac D, Molnar V, Rod E, et al. Knee osteoarthritis: a review of pathogenesis and state-of-the-art non-operative therapeutic considerations. *Genes*. 2020;11(8):854. doi:10.3390/genes11080854
11. Vigotsky AD, Cong O, Pinto CB, et al. Prognostic value of preoperative mechanical hyperalgesia and neuropathic pain qualities for postoperative pain after total knee replacement. *Eur J Pain*. 2024;28(8):1387–1401. doi:10.1002/ejp.2295
12. Lim WB, Al-Dadah O. Conservative treatment of knee osteoarthritis: a review of the literature. *World J Orthoped*. 2022;13(3):212–229. doi:10.5312/wjo.v13.i3.212
13. Yetişir A, Öztürk GY. Effects of low-level laser therapy on acupuncture points on knee pain and function in knee osteoarthritis. *Rev Assoc Med Bras*. 2024;70(1). doi:10.1590/1806-9282.20230264

14. Henderson LA, Canna SW, Friedman KG, et al. American college of rheumatology clinical guidance for pediatric patients with Multisystem Inflammatory Syndrome in Children (MIS-C) associated with SARS-CoV-2 and hyperinflammation in COVID-19. version 1. *Arthritis Rheumatol*. 2020;72(11):1791–1805. doi:10.1002/art.41454
15. Tu J, Wang L, Shi G, et al. Effect of acupuncture on knee injury and osteoarthritis outcome score in patients with knee osteoarthritis. *Chin Acupunct Moxibustion*. 2021;41(01):27–30. doi:10.13703/j.0255-2930.20191212-0001
16. Peng K, Guo X, Huang Z, Xu D. Observations on the analgesic effect of electroacupuncture of different duration on knee osteoarthritis. *Shanghai J Acupunct Moxibustion*. 2022;41(10):1011–1015. doi:10.13460/j.issn.1005-0957.2022.10.1011
17. Deng R, Zhao R, Zhang Z, et al. Chondrocyte membrane–coated nanoparticles promote drug retention and halt cartilage damage in rat and canine osteoarthritis. *Sci, trans med*. 2024. doi:10.1126/scitranslmed.adh9751
18. Zhang W, Zhang L, Yang S, Wen B, Chen J, Chang J. Electroacupuncture ameliorates knee osteoarthritis in rats via inhibiting NLRP3 inflammasome and reducing pyroptosis. *Mol Pain*. 2022. doi:10.1177/17448069221147792
19. Liu S, Chen Q, Zhang Q, et al. Electroacupuncture combined with extracorporeal shock wave therapy improves pain symptoms and inflammatory factor levels in knee osteoarthritis patients. *Heliyon*. 2023. doi:10.1016/j.heliyon.2023.e20771
20. Huang H, Liang Y, Han D, Chen X, Xiao L, Wu H. Case report: electroacupuncture for acute pain flare-up of knee osteoarthritis. *Front Neurol*. 2022. doi:10.3389/fneur.2022.1026441
21. Xing L, Chen X, Guo C, et al. Electroacupuncture exerts chondroprotective effect in knee osteoarthritis of rabbits through the mitophagy pathway. *J Pain Res*. 2023;Volume 16:2871–2882. doi:10.2147/jpr.s416242
22. Tong J, Deng C, Sun G, et al. Electroacupuncture upregulates HIF-1α and SOX9 expression in knee osteoarthritis. *Evid Based Complement Alternat Med*. 2021;2021:1–9. doi:10.1155/2021/2047097
23. Wang C, Xu M, Zuo W, et al. Effects of electroacupuncture combined with Chinese herbal extract on pain behavior, osteoclast differentiation and Hedgehog signaling pathway in rats with rheumatoid arthritis. *Chin J Rehab*. 2023;38(11):643–648.
24. Sasaki Y, Kijima K, Yoshioka K. Validity evaluation of a rat model of monoiodoacetate-induced osteoarthritis with clinically effective drugs. *BMC Musculoskelet Disord*. 2024;25(1). doi:10.1186/s12891-024-08083-9
25. Oka Y, Murata K, Ozone K, et al. Mild treadmill exercise inhibits cartilage degeneration via macrophages in an osteoarthritis mouse model. *Osteoarthr Cartil Open*. 2023;5(2):100359. doi:10.1016/j.ocarto.2023.100359
26. Wu Z. Clinical application of yanglingquan acupoint. *Adv Clin Med*. 2023. doi:10.12677/acm.2023.1361245
27. Li S, Li J, Yan W. Analysis of clinical acupoint selection rules in acupuncture treatment of knee osteoarthritis based on data mining technology. *Chin Imag J Integr Tradit Western Med*. 2021;19(03):210–216.
28. Griffioen MA, Dernetz VH, Yang GS, Griffith KA, Dorsey SG, Renn CL. Evaluation of dynamic weight bearing for measuring nonevoked inflammatory hyperalgesia in mice. *Nurs Res*. 2015;64(2):81–87. doi:10.1097/nnr.0000000000000082
29. Yau LIK, Henry FU, Man Hong C, et al. Swelling assessment after total knee arthroplasty. *J Orthop Surg*. 2022;30(3). doi:10.1177/10225536221127668
30. Lu F, Kato J, Toramaru T, Sugai M, Zhang M, Morisaki H. Objective and quantitative evaluation of spontaneous pain-like behaviors using dynamic weight-bearing system in mouse models of postsurgical pain. *J Pain Res*. 2022;15:1601–1612. doi:10.2147/jpr.S359220
31. Westhof A, Kleinschmidt-Doerr K, Michaelis M, Brenneis C. Dynamic weight-bearing test during jumping: a sensitive outcome measure of chronic osteoarthritis pain in rats. *Heliyon*. 2021;7(9):e07906. doi:10.1016/j.heliyon.2021.e07906
32. Wang Z, Xu H, Wang Z, et al. Effects of externally-applied, non-pharmacological Interventions on short- and long-term symptoms and inflammatory cytokine levels in patients with knee osteoarthritis: a systematic review and network meta-analysis. *Front Immunol*. 2023;14. doi:10.3389/fimmu.2023.1309751
33. Yu D, Xu J, Liu F, Wang X, Mao Y, Zhu Z. Subchondral bone changes and the impacts on joint pain and articular cartilage degeneration in osteoarthritis. *Clin Exp Rheumatol*. 2016;34(5):929–934.
34. Oláh T, Cucchiarini M, Madry H. Subchondral bone remodeling patterns in larger animal models of meniscal injuries inducing knee osteoarthritis – a systematic review. *Knee Surg Sports Traumatol Arthrosc*. 2023;31(12):5346–5364. doi:10.1007/s00167-023-07579-6
35. Lin J, Wu G, Chen J, et al. Electroacupuncture inhibits sodium nitroprusside-mediated chondrocyte apoptosis through the mitochondrial pathway. *Mol Med Rep*. 2018. doi:10.3892/mmr.2018.9498
36. Qiao J, Guo X, Zhang L, Zhao H, He X. Autologous platelet rich plasma injection can be effective in the management of osteoarthritis of the knee: impact on IL-1 β, TNF-α, hs-CRP. *J Orthopaedic Surg Res*. 2024;19(1). doi:10.1186/s13018-024-05060-9
37. Chen P, Xu H, Zhang R, X-s T. Dose-effect relationship between electroacupuncture with different parameters and the regulation of endogenous opioid peptide system ☆. *World J Acupunct - Moxibustion*. 2023. doi:10.1016/j.wjam.2023.06.003
38. Lin J-G, Kotha P, Chen Y-H. Understandings of acupuncture application and mechanisms. *Am J Transl Res*. 2022;14(3):1469–1481.
39. Zhongheng DU, Wenjie C, Kejing T, et al. Electroacupuncture stimulating Zusanli (ST36), Sanyinjiao (SP6) in mice with collagen-induced arthritis leads to adenosine A2A receptor-mediated alteration of p38α mitogen-activated protein kinase signaling and inhibition of osteoclastogenesis. *J Traditional Chin Med*. 2023;43(6):1103–1109. doi:10.19852/j.cnki.jtcm.2023.06.001
40. Wang Z, Yuan M, Chen X, et al. Electroacupuncture alleviates MIA-induced pain via suppressing P2X4 expression in a rat model of knee osteoarthritis. *Osteoarthritis Cartilage*. 2021;29:S369. doi:10.1016/j.joca.2021.02.479
41. Chen W, Zhang X-N, Su Y-S, et al. Electroacupuncture activated local sympathetic noradrenergic signaling to relieve synovitis and referred pain behaviors in knee osteoarthritis rats. *Front Mol Neurosci*. 2023;16. doi:10.3389/fnmol.2023.1069965
42. Bai F, Ma Y, Guo H, et al. Spinal cord glycine transporter 2 mediates bilateral st35 acupoints sensitization in rats with knee osteoarthritis. *Evid Based Complement Alternat Med*. 2019;2019:1–17. doi:10.1155/2019/7493286
43. Cai F, Li F, Zhang Y, Li P, Xiao B. Research on electroacupuncture parameters for knee osteoarthritis based on data mining. *Eur J Med Res*. 2022;27(1). doi:10.1186/s40001-022-00795-9